Available online at www.sciencedirect.com
SCIENCE DIRECT®
Acta Materialia 53 (2005) 4567–4578
Acta MATERIALIA
www.actamat-journals.com

Crystallization and creep behavior of Si–B–C–N ceramics

N.V. Ravi Kumar [a,*], Sabine Prinz [a], Ye Cai [a,1], André Zimmermann [a,2], Fritz Aldinger [a], Frank Berger [b], Klaus Müller [b,*]

[a] *Max-Planck-Institut für Metallforschung and Institut für Nichtmetallische Anorganische Materialien, Universität Stuttgart, Pulvermetallurgisches Laboratorium, Heisenbergstrasse 3, D-70569, Stuttgart, Germany*
[b] *Institut für Physikalische Chemie, Universität Stuttgart, Pfaffenwaldring 55, D-70569, Stuttgart, Germany*

Received 22 August 2004; received in revised form 22 April 2005; accepted 8 June 2005
Available online 8 August 2005

Abstract

Amorphous Si–B–C–N ceramics were prepared from suitable boron-modified polyvinylsilazanes by solid state thermolysis under an argon atmosphere. The amorphous Si–B–C–N ceramics were further annealed at 1800 °C by applying different nitrogen pressures and holding times. The present work reports for the first time on high temperature creep studies coupled with a comprehensive structural characterization of the samples via X-ray diffraction, transmission electron microscopy and solid state NMR methods. It is shown that, depending on the actual annealing conditions, SiC and Si_3N_4 nanocrystallites are formed which are distributed in an amorphous B–C–N matrix consisting of amorphous carbon and boron nitride domains. The high temperature mechanical properties of the various annealed Si–B–C–N samples and of a representative amorphous specimen were examined by compression creep experiments. Constant load experiments were carried out at 1400 °C which showed that an improved creep resistance exists for the annealed Si–B–C–N samples, containing SiC and Si_3N_4 nanocrystallites. The smaller creep rates of the nanocrystalline ceramic are attributed primarily to the densification of the amorphous structure upon sample annealing. In addition, load change experiments were performed on the present ceramic materials. The high temperature viscosities derived were found to be substantially higher than for instance those discussed for fused silica. Finally, the anelastic behavior was examined by load release experiments. Here, a quantification of the experimental data was possible on the basis of the Kohlrausch–Williams–Watts equation.

Keywords: Nanocrystalline Si–B–C–N ceramics; Solid state NMR; TEM; Compression creep; Viscosity; Anelasticity; KWW

1. Introduction

Precursor-derived Si–B–C–N ceramics have attracted considerable interest in recent years primarily because of their extraordinary material properties [1,2]. It has been demonstrated that the addition of boron to ternary Si–C–N ceramics results in a substantial increase of the thermal stability of these materials. Thus, Si–B–C–N ceramics were reported to be stable up to temperatures of 2000 °C [3–6]. In the past, studies about the mechanical properties were mainly focused on the amorphous state of the precursor-derived ceramics. For instance, compression creep studies on amorphous Si–C–N and Si–B–C–N ceramics in the temperature range from 1400 to 1550 °C at stresses between 30 and 250 MPa demonstrated that these materials exhibit an unusually high creep resistance [7]. Likewise, deformation models – developed for metallic glasses – were employed for the description of the deformation behavior in

* Corresponding authors. Tel.: +49 711 6893108; fax: +49 711 6893131 (N.V. Ravi Kumar), Tel.: +49 711 685 4470; fax: +49 711 685 4467 (K. Müller).
E-mail addresses: kumar@mf.mpg.de (N.V. Ravi Kumar), k.mueller@ipc.uni-stuttgart.de (K. Müller).
[1] Present address: Department of Materials Science and Engineering, Georgia Institute of Technology, USA.
[2] Present address: Robert Bosch GmbH, Corporate Research and Development, Stuttgart, Germany.

1359-6454/$30.00
doi:10.1016/j.actamat.2005.06.011

amorphous Si–B–C–N ceramics which provided new insights into the mechanical properties of these materials [8]. Apart from an earlier examination of the deformation behavior of crystallized Si–B–C–N ceramics [9], a comprehensive study about the effect of crystallization on the mechanical properties of such quaternary ceramics has not been reported so far.

For this reason, we report in the present work on compression creep investigations of annealed Si–B–C–N ceramic samples, derived via thermolysis of a suitable boron-modified polyvinylsilazane precursor. In order to examine the influence of the actual annealing condition on the structure of the final Si–B–C–N ceramics, the respective (intermediate) amorphous samples were heat-treated employing different annealing conditions, i.e., nitrogen pressure and annealing time. A comprehensive structural characterization of the annealed Si–B–C–N specimens was achieved by the combined application of X-ray diffraction (XRD), solid-state NMR spectroscopy and transmission electron microscopy (TEM). It was found that in particular the amount of SiC and Si_3N_4 nanocrystallites strongly depends on the chosen experimental conditions. The high temperature deformation behavior was examined via constant load and load change experiments at 1400 °C on both annealed Si–B–C–N ceramics and the as-pyrolyzed amorphous ceramic prior to further crystallization. The results from the present mechanical studies are discussed in connection with the specific structural features of these quaternary ceramic materials.

2. Experimental

2.1. Sample preparation

The synthesis of the polymer precursor – a boron-modified polyhydridovinylsilazane with a chemical composition $(B[C_2H_4\text{-}Si(H)NH]_3)_n$ – from which the Si–B–C–N ceramic was prepared is described elsewhere [4]. The solid polymer was milled and sieved. The resulting particles were segregated into various size fractions, which were then thoroughly mixed in various proportions. In the next step, the polymer particles were compacted to yield a green body by uniaxial warm-pressing in a graphite die at a pressure of 48 MPa within a temperature range of 150–350 °C. The thermolysis of the green body was carried out in an argon atmosphere by heating at a rate of 1 K/min to 1400 °C, keeping the sample at this temperature for 2 h, and cooling back to room temperature at a cooling rate of 5 K/min. During this thermal treatment a series of solid state transformations (i.e., ceramization reactions) take place along with the evolution of different gaseous species. As a result, the polymer precursor is converted into the desired amorphous ceramic (Si–B–C–N ceramic). The amorphous ceramic was then annealed at 1800 °C at a nitrogen pressure between 10 and 100 bar, and at holding times between 1 and 3 h, in order to crystallize the metastable as-pyrolyzed material. In the present work, four different annealed Si–B–C–N specimens were prepared which refer to the following treatments: (i) 1 h, 10 bar N_2 (sample **I**), (ii) 3 h, 10 bar N_2 (sample **II**), (iii) 1 h, 100 bar N_2 (sample **III**), and (iv) 3 h, 100 bar N_2 (sample **IV**). For comparison, experimental data will also be provided for the amorphous Si–B–C–N ceramic (sample **V**), which reflects the situation right after thermolysis of the green body to 1400 °C, as described above.

2.2. Solid-state NMR spectroscopy

Solid-state NMR experiments were carried out at room temperature on a Bruker MSL spectrometer operating at a static magnetic field of 7.05 T (^{1}H frequency: 300.13 MHz) using a 4 mm magic angle spinning (MAS) probe. ^{13}C, ^{29}Si and ^{11}B NMR experiments were performed at 75.47, 59.6 and 96.26 MHz, respectively. ^{13}C and ^{29}Si NMR spectra were recorded under MAS conditions (sample rotation frequency: 5 kHz) with single pulse excitation, using $\pi/2$ pulse widths of 4.0 μs (^{13}C, ^{29}Si) and recycle delays up to 5 min. ^{29}Si and ^{13}C chemical shifts were determined relative to external standards Q_8M_8 (trimethylsilylester of octameric silicate) and adamantane, respectively. These values were then expressed relative to the reference compound TMS ($\delta = 0$ ppm). ^{11}B MAS NMR (central transition) spectra were recorded at a sample spinning rate 10 kHz with single pulse excitation using $\pi/6$ (pulse length: 1.2 μs) pulses and a recycle delay of 2 s. The spectra were calibrated relative to an aqueous solution of H_3BO_3 ($\delta =$ 19.6 ppm) as the external standard and are given relative to $BF_3 \cdot OEt_2$ ($\delta = 0$ ppm).

2.3. X-ray diffraction

The X-ray diffraction measurements were carried out at room temperature on a Siemens D5000 X-ray diffractometer with a position-sensitive detector. The voltage and current used for the measurements were 40 kV and 30 mA, respectively.

2.4. TEM experiments

The samples used for the TEM experiments from Si–B–C–N ceramics **I**–**IV** were prepared following standard techniques, which involve diamond cutting, ultrasonic drilling, mechanical grinding, dimpling, polishing, and argon-ion thinning to perforation. TEM measurements at room temperature were carried out using a Philips CM200 microscope at an operating voltage of 200 kV. It should be noted that the corresponding TEM image of sample **III** could not be given due to

Table 1
Experimental conditions for load change experiments

Time (s)	Stress (MPa)
$0–2.5\times10^5$	100
$2.5\times10^5–5\times10^5$	150
$5\times10^5–9\times10^5$	200
$9\times10^5–1\times10^6$	5

its poor quality (the reason for that is not known so far), and because, due to decomposition of the sample, the experiment could not be repeated again.

2.5. Mechanical measurements

Creep specimens with nominal dimensions of 3 mm × 3 mm × 7 mm were cut from the ceramic monoliths followed by grinding. Compression creep tests in air were performed at 1400 °C coupled with a compressive stress of 100 MPa for constant load experiments for all four annealed (crystallized) Si–B–C–N samples. Load change experiments were conducted with the conditions summarized in Table 1. For comparison, measurements were made on the respective amorphous Si–B–C–N sample. The compression creep experiments were carried out using a testing frame from Amsler, covering a force range between 0.5 and 5 kN (accuracy: 1 N). The temperature was measured with a Pt-Rh(10)/Pt thermocouple. The load was applied by a spiral spring, which was preloaded by a spindle. The compression of the spiral spring was measured by a linear potentiometer. The strain of the specimen was calculated from the displacement of the load pads. Two SiC scanning pins connected the upper load pad with the housing of an inductive strain gauge, which was placed under the specimen outside of the furnace in the cold part of the testing machine. The displacement between the upper and lower load pad was measured with a third scanning pin, which connected the sensor of the strain gauge with the lower load pad.

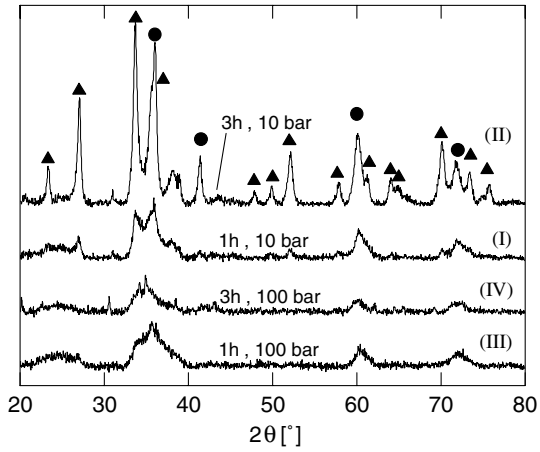

Fig. 1. X-ray diffraction pattern of four different Si–B–C–N samples, annealed at 1800 °C with the conditions (holding time, N_2 pressure) described in the text (●: α/β-SiC, ▲: β-Si_3N_4).

3. Results

3.1. Structural characterization

The X-ray diffraction diagrams of the Si–B–C–N ceramics obtained by annealing at 1800 °C for different holding times and nitrogen pressures are given in Fig. 1. They reflect a considerable influence of the nitrogen pressure on the crystallization of the present amorphous Si–B–C–N ceramics. Obviously, a high nitrogen pressure of 100 bar retards the crystallization process. Here, the corresponding samples with 1 and 3 h of annealing (samples **III** and **IV**) exhibit only three broad peaks at $2\theta = 36°$, 60.5°, and 72°, due to the formation of some silicon carbide domains. If during the annealing

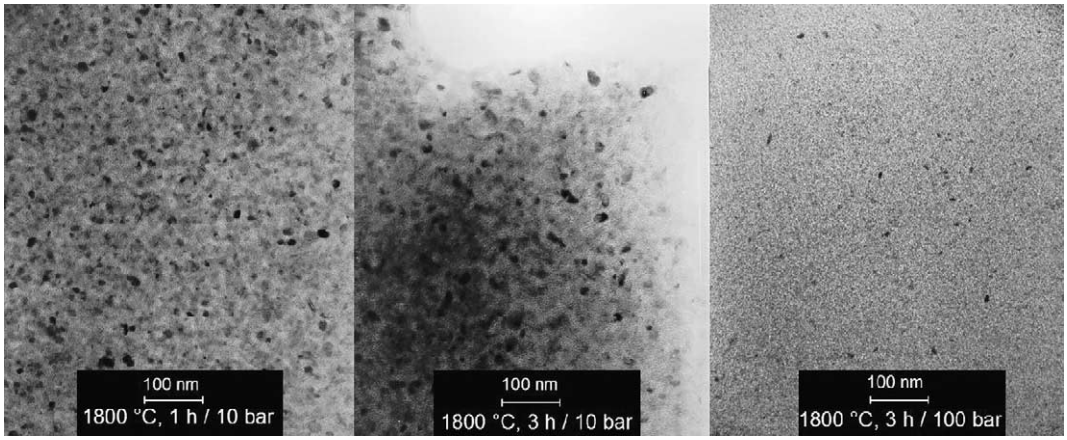

Fig. 2. TEM images of nano-crystalline Si–B–C–N ceramics crystallized at 1800 °C, 1 h/10 bar N_2 pressure (sample **I**), 1800 °C, 3 h/10 bar N_2 pressure (sample **II**) and 1800 °C, 3 h/100 bar N_2 pressure (sample **IV**).

process a lower nitrogen pressure of 10 bar is applied, then additional peaks due to the formation of silicon nitride are visible. At a holding time of 1 h (sample **I**) only relatively weak and broad diffraction signals show up. An extension of the holding time to 3 h, however, results in a considerable sharpening of all reflections along with a substantial increase of the peak intensities (sample **II**).

The bright-field TEM images of crystalline Si–B–C–N ceramics, obtained at nitrogen pressures of 10 and 100 bar (samples **I**, **II** and **IV**), are presented in Fig. 2. The TEM images of the specimen **I** and **II**, obtained at 10 bar N_2 clearly proves the formation of SiC and Si_3N_4 nanocrystallites. The mean crystallite size is estimated to be 30 nm for sample **II**. The TEM image for samples obtained at a higher nitrogen pressure of 100 bar and an annealing time of 3 h (sample **IV**) reflect suppression of crystallization as a result of application of higher nitrogen pressure, in close agreement with the findings from the X-ray diffraction experiments (see above, Fig. 1).

The experimental solid-state ^{13}C NMR spectra of the same materials, derived from boron-modified polyhydridovinylsilazane under different annealing conditions, are given in the left column of Fig. 3. The upper spectrum, referring to sample **I** (annealing time: 1 h, nitrogen pressure: 10 bar) exhibits two broad signals at around 120 and 20 ppm, which, according to previous studies on boron-modified polysilazanes [10,11], can be attributed to amorphous (graphite-like) carbon and $\mathbf{C}H_xSi_{4-x}$ units ($x = 0$, 1 or 2), respectively. A longer annealing

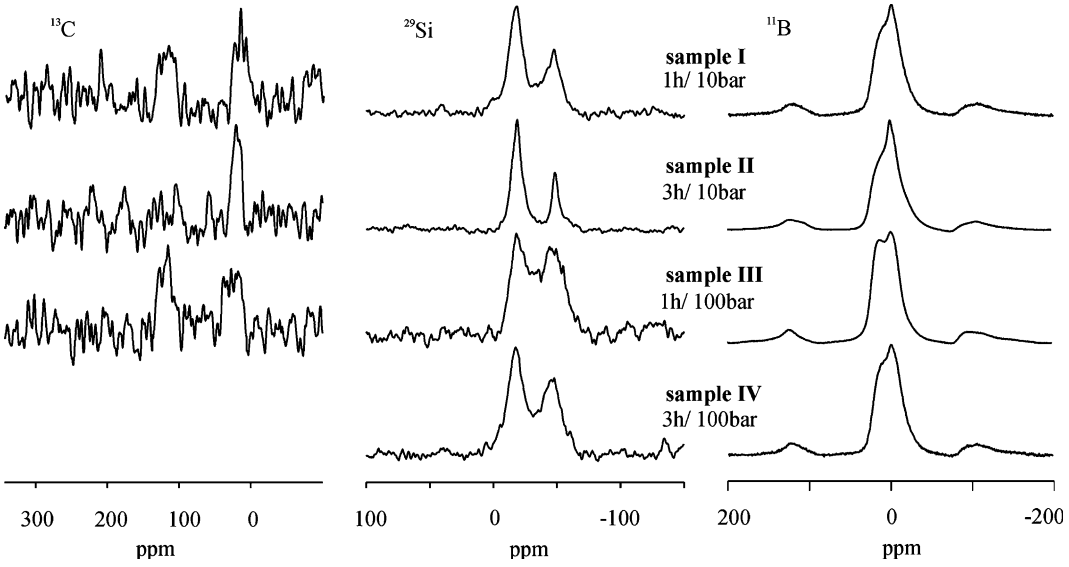

Fig. 3. ^{13}C (left), ^{29}Si (middle) and ^{11}B NMR spectra (right) of four different Si–B–C–N samples, annealed at 1800 °C with the conditions (holding time, N_2 pressure) described in the text.

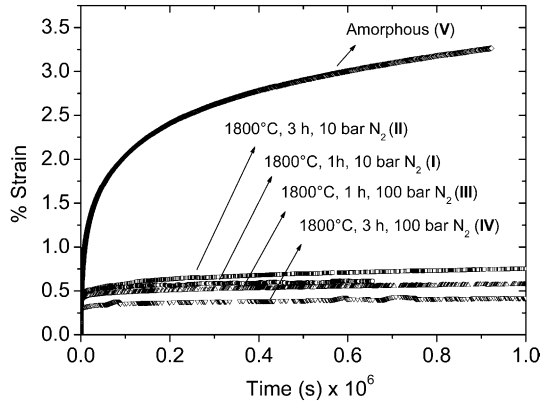

Fig. 4. Deformation curves of four different Si–B–C–N samples, annealed at 1800 °C with the conditions (holding time, N_2 pressure) described in the text, and of the corresponding amorphous specimen. The experiments were performed at 1400 °C with a compressive stress of 100 MPa.

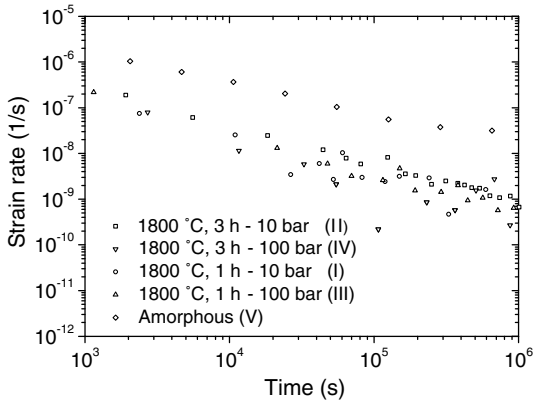

Fig. 5. Deformation rates for annealed Si–B–C–N samples and for the corresponding amorphous specimen, derived from constant load experiments (see Fig. 4). The experiments were performed at 1400 °C with a compressive stress of 100 MPa.

time of 3 h (sample **II**) at the same nitrogen pressure gives rise to a ^{13}C NMR spectrum (second spectrum from the top) with a single peak in the high field region at 20 ppm. The ^{13}C NMR spectrum for the sample annealed at a nitrogen pressure of 100 bar (annealing time: 1 h, sample **III**) again contains both signals at 120 and 20 ppm, as discussed for sample **I**. In the case of 3 h annealing at a nitrogen pressure of 100 bar (sample **IV**) no ^{13}C NMR signals could be detected, which on the basis of former studies, however, is not unusual. In fact, other NMR studies on such precursor-derived ceramics have shown that in general ^{13}C NMR spectra are very difficult to detect at annealing temperatures beyond 1100 °C [10,11]. The ^{13}C NMR spectra shown here

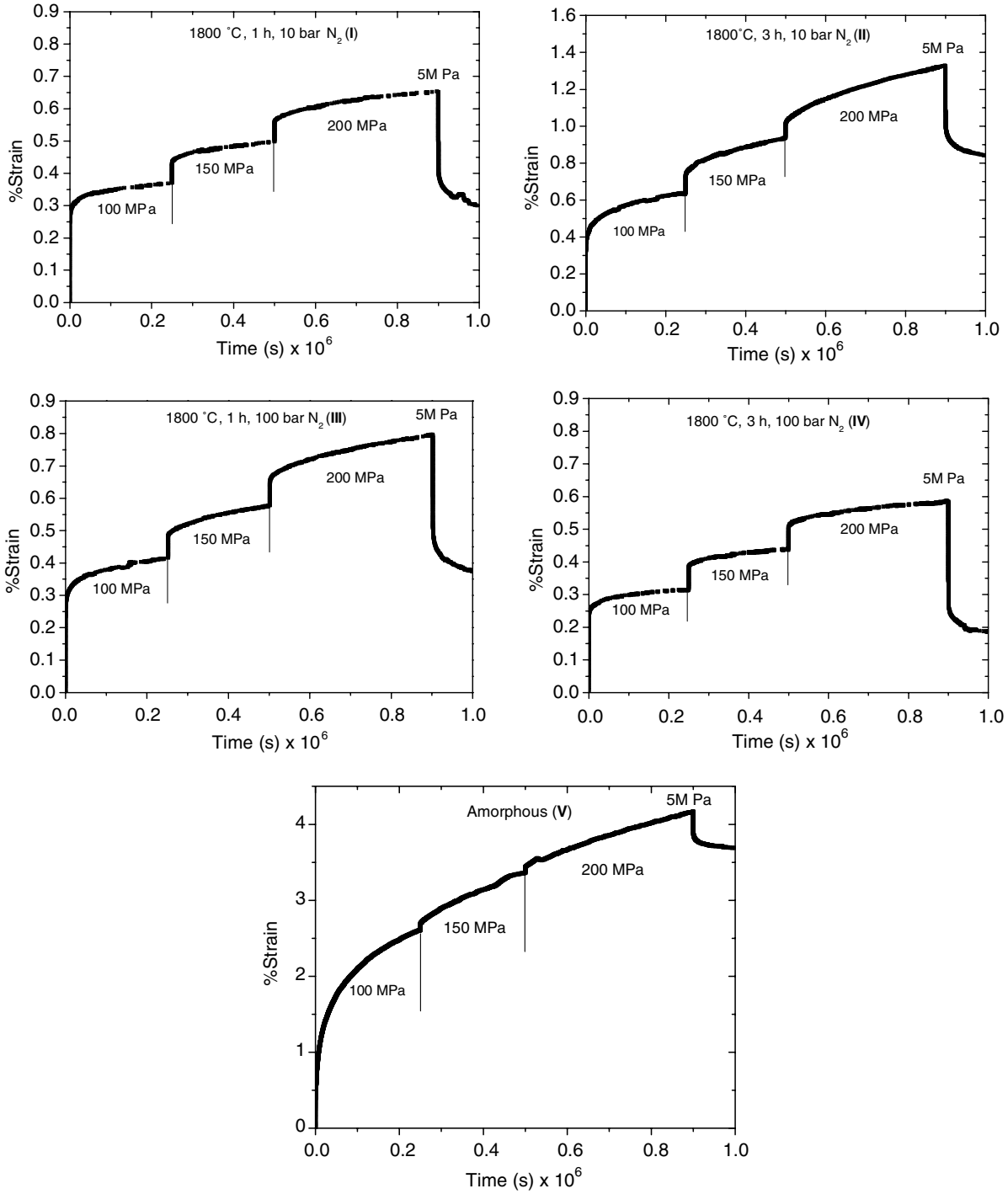

Fig. 6. Deformation (strain) as a function of time for nano-crystalline Si–B–C–N ceramics and amorphous Si–B–C–N ceramics during load change experiments at 1400 °C.

therefore represent rare cases, where it was nevertheless possible to get ^{13}C NMR signals of reasonable quality.

The corresponding ^{29}Si NMR spectra are given in the second column of Fig. 3. Inspection of these spectra reveals that, independent of the particular annealing conditions, two signals can be registered at −18 and −48 ppm, which are attributed to the formation of SiC_4 (β-SiC: −20 ppm [12]) and SiN_4 units (Si_3N_4: −48 ppm [13]), respectively. The relative magnitudes and widths of these signals, however, vary with the actual annealing conditions. It is quite obvious that the ^{29}Si NMR signals from samples **I** and **II** exposed to a lower nitrogen pressure of 10 bar exhibit a smaller line width than those obtained from treatment at higher nitrogen pressure. Likewise, the relative signal intensity of the SiN_4 units is found to increase with increasing nitrogen pressure, and decreases with increasing annealing time, whereas the signal intensity of the SiC_4 units displays the opposite behavior.

The signals derived from the samples annealed at the higher nitrogen pressure clearly show an increased intensity in between the two peaks of SiC_4 and SiN_4 which indicates the presence of mixed coordinated silicon atoms, i.e., SiC_3N, SiC_2N_2 and $SiCN_3$ units, typical for the amorphous state of such materials. According to these data, sample **III** annealed for only 1 h contains the highest amount of amorphous phase.

The experimental ^{11}B NMR spectra are displayed in the right column of Fig. 3. These spectra consist of two components: (i) a broad spectral component with a second-order quadrupolar broadening, which is typical for trigonally coordinated boron (BN_3 units [14]) as in hexagonal boron nitride, and (ii) a second, isotropic signal at 0 ppm which can be attributed to tetragonally co-ordinated boron (BN_4 units [14]). The former component obviously dominates the ^{11}B NMR spectrum of sample **III** (annealing conditions: 1 h/100 bar N_2). The isotropic component is found to increase with increasing annealing time and upon lowering the nitrogen pressure.

In summary, the present X-ray, solid-state NMR and TEM data seem to provide consistent results for the various samples, as will be further discussed below. The microstructure of the annealed samples is characterized by small crystallites embedded in a matrix phase which is still amorphous. The highest amount of crystallinity was detected for sample **II**, with a mean crystallite size of about 30 nm. A further quantification of the amount of crystalline phases in the present samples, however, was not feasible.

3.2. Constant load experiments

Compression creep experiments were performed for the aforementioned Si–B–C–N specimens, obtained with four different annealing treatments. The experiments were done at a temperature of 1400 °C, and with a compression load of 100 MPa. For comparison, a representative amorphous Si–B–C–N ceramic sample (i.e., without high-temperature annealing) was examined employing the same experimental conditions. The results are summarized in Fig. 4. In contrast to normal conventions, the positive strain in Fig. 4 denotes compression in the direction of the applied load. It can be seen that the deformation curves of samples **I**–**IV** behave in a very similar way and quite different from that recorded for the amorphous sample.

In Fig. 5 the deformation rates $\dot{\varepsilon}$ for the annealed samples **I**–**IV** are depicted along with those from the amorphous counterpart (sample **V**). It can be seen that the time dependence of $\dot{\varepsilon}$ for the amorphous and annealed, nanocrystalline ceramics is almost identical, including the absence of any asymptotic behavior even after 300 h of testing time. However, there is a considerable difference between the annealed and the amorphous Si–B–C–N samples, as the former display a significant increase of their creep resistance. The annealed material therefore exhibits deformation rates $\dot{\varepsilon}$, which are about one order of magnitude smaller than those of the amorphous counterpart (sample **V**) throughout the whole testing time covered here. At the same time, for the annealed, nanocrystalline ceramics the deformation rates $\dot{\varepsilon}$ decrease by about $2\frac{1}{2}$ orders of magnitude reaching a value of 10^{-9} 1/s after 300 h at the end of the constant load experiment. It is worth noting that although sample **II** seems to be structurally somewhat different from the other three annealed specimens (higher amount of crystallinity, i.e. Bragg reflections indicated clearly the presence of SiC and Si_3N_4), very similar strain rates (or the scatter in the data) were obtained for all four annealed Si–B–C–N samples.

3.3. Load change experiments

Additional compression creep experiments, by applying various loads between 5 and 200 MPa at the time

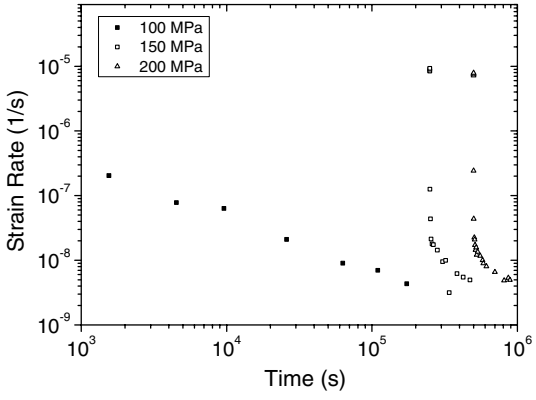

Fig. 7. Deformation rates as a function of time for an annealed Si–B–C–N sample (sample **II**), derived from load change experiments at 1400 °C (see Fig. 6).

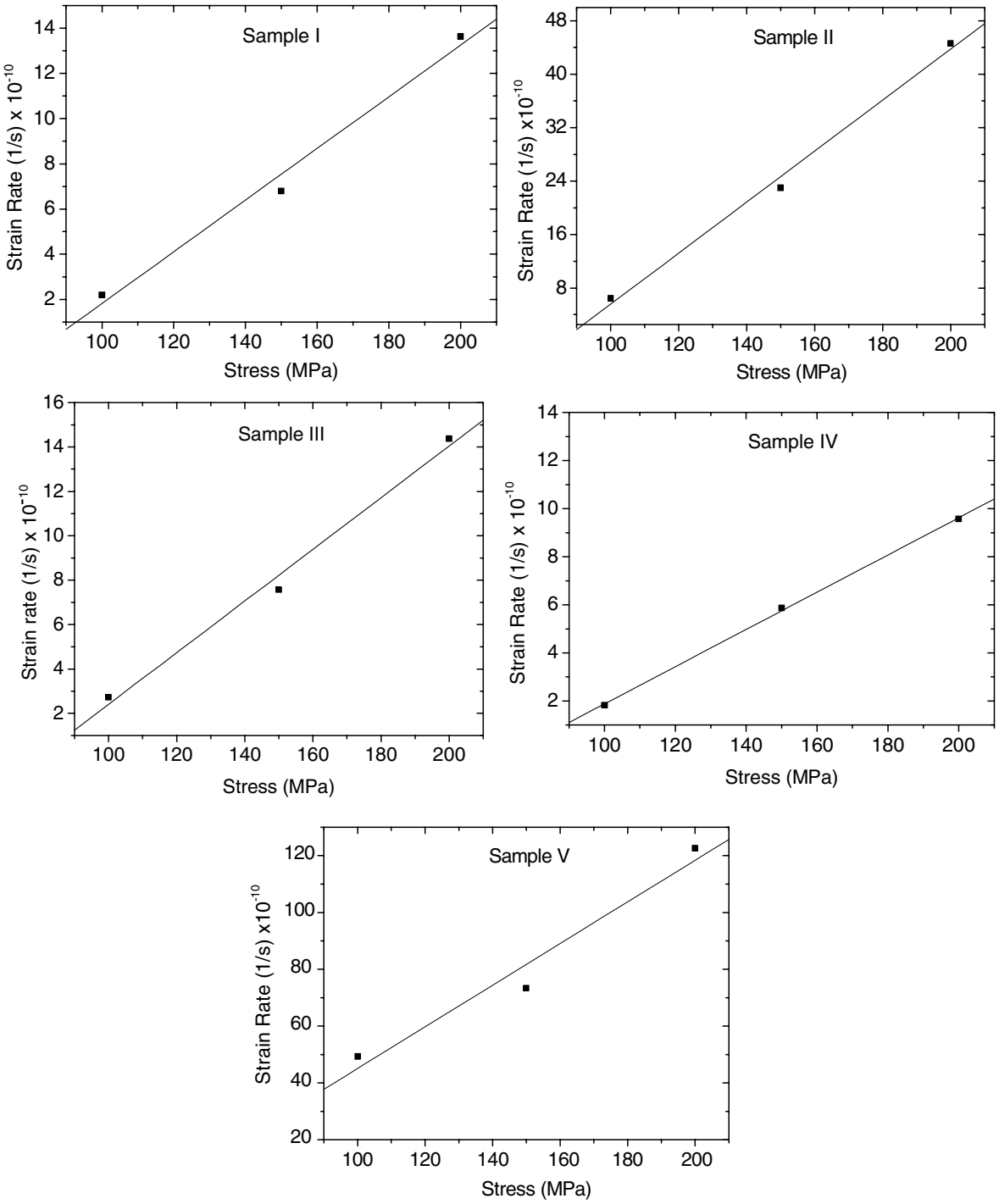

Fig. 8. Deformation rates for annealed Si–B–C–N samples and the corresponding amorphous specimen as a function of the applied stress, derived from load change experiments at 1400 °C (see Fig. 6).

intervals given in Table 1, were performed for the aforementioned annealed, nanocrystalline Si–B–C–N ceramics **I**–**IV** and the corresponding amorphous sample **V**. The dependence of the deformation as a function of increasing load (100–200 MPa) is shown in Fig. 6. At the end of the experiment the samples were unloaded from 200 MPa to 5 MPa, from which further information about the anelastic behavior in these materials

Table 2
Calculated creep viscosities obtained from load change experiments

Material condition	Viscosity
Amorphous	4.50×10^{15} Pa s
1800 °C, 3 h, 10 bar N_2 (**II**)	8.72×10^{15} Pa s
1800 °C, 3 h, 100 bar N_2 (**IV**)	4.31×10^{16} Pa s
1800 °C, 1 h, 10 bar N_2 (**I**)	2.96×10^{16} Pa s
1800 °C, 1 h, 100 bar N_2 (**III**)	2.86×10^{16} Pa s

was expected. In Fig. 7 representative deformation rates $\dot{\varepsilon}$ are given for sample **II**, which were derived from the curves in Fig. 6.

Inspection of the data in Figs. 6 and 7 reveals that the deformation rates continue to decrease even after 300 h of testing time which holds for the amorphous and nanocrystalline ceramics as well as for all applied loads. Hence, the strain rate $\dot{\varepsilon}$ of the crystallized material can be approximated by Eq. (1), which was earlier applied for the description of strain rate curves from amorphous precursor-derived ceramics [9,15]

$$\dot{\varepsilon} = \frac{1}{a + bt}. \tag{1}$$

In this equation a and b are fitting parameters, while t represents the creep time.

The viscosities of the present ceramic materials were determined by plotting the deformation rates $\dot{\varepsilon}$ as a function of applied stress σ, and assuming Newtonian viscous flow (see Fig. 8). The values of the deformation rates $\dot{\varepsilon}$ for various loads (i.e., stresses σ) at an identical time of $t = 10^6$ s were obtained by extrapolation of the data given in Fig. 7. The viscosity η is calculated by means of the following equation:

$$\eta = \frac{\sigma}{3 \cdot \dot{\varepsilon}}. \tag{2}$$

The derived viscosities from this analysis are summarized in Table 2. It can be seen that the viscosities of the annealed, nanocrystalline samples are about one order of magnitude larger than that of the amorphous sample **V**. However, this is a relatively small difference, unlike the findings, for instance, in metallic glasses [16–18].

If during a load experiment the load on the specimen is released, then a finite time is required to establish equilibrium between stress and strain in the unloading direction. The resulting time-dependent reversible deformation, which also depends on the applied initial stress, is termed anelastic. In fact, such an anelastic deformation was observed earlier for amorphous precursor-derived Si–B–C–N ceramics [19]. We have performed such an unloading experiment for the present materials by reducing the load from 200 to 5 MPa (see Fig. 6). The time dependence of the anelastic strain rates for the amorphous and nanocrystalline Si–B–C–N ceramics (sample **II**) is given in a double logarithmic representation in Fig. 9.

These experimental data were fitted using the well-known Kohlrausch–Williams–Watts (KWW) equation, which is frequently used for the description of relaxation processes in various materials [20–24]. According to this approach, the relaxation for a residual strain $\varepsilon(t)$ is described by the following equation:

$$\dot{\varepsilon} = \frac{\mathrm{d}\varepsilon(t)}{\mathrm{d}t} = -\gamma(t) \cdot \varepsilon(t). \tag{3}$$

The time dependence of the coefficient $\gamma(t)$ is assumed to follow

$$\gamma \propto t^{-(1-\beta)} \quad \text{with } 0 < \beta \leqslant 1. \tag{4}$$

The analytical solution of Eq. (4) is known as the stretched exponential or KWW function [25]. The anelastic strain $\varepsilon_{\mathrm{an}}(t, T)$ is then given by

$$\varepsilon_{\mathrm{an}}(t, T) = \varepsilon_0 \exp\left[-\left(\frac{t}{\tau_{\mathrm{rel}}(T)}\right)^{\beta}\right]. \tag{5}$$

The parameter τ_{rel} in Eq. (5) denotes an effective relaxation time, while the stretching exponent β quantifies the extent of deviation from pure exponentiality, or equivalently, the degree of relaxation time dispersion. The KWW function implies a spectrum of relaxation times whose width is connected with the parameter β. A stretching exponent β of 1 thus describes a relaxation process with a single activation energy (infinitesimally sharp relaxation spectrum), while the relaxation spectrum broadens to an indefinite number of activation energies for values of β close to zero [26]. The time deriv-

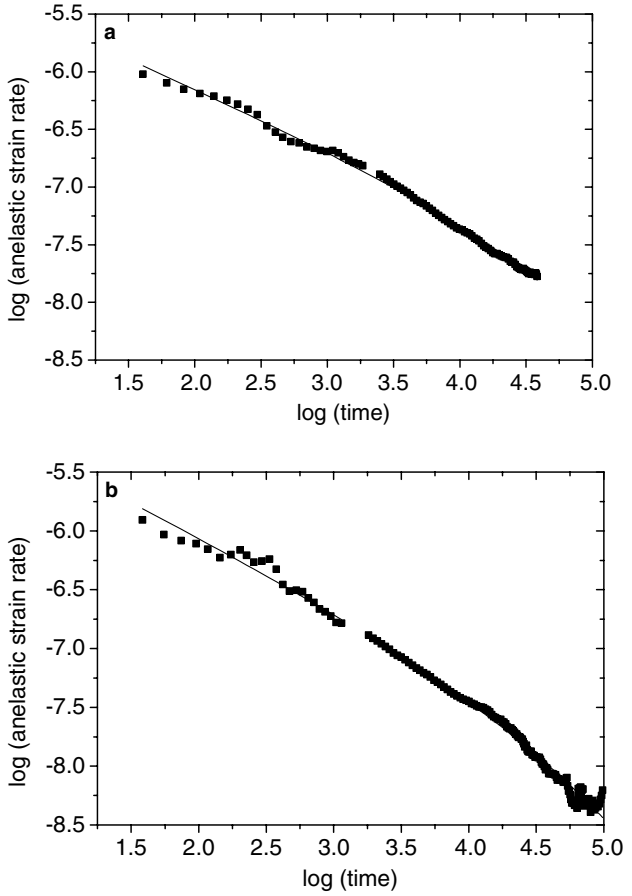

Fig. 9. Experimental deformation rates as a function of time, derived from load release experiments at 1400 °C (see Fig. 6). The theoretical fits using the Kohlrausch–Williams–Watts equation are also given. The two diagrams refer to (a) the amorphous (sample **V**) and (b) an annealed Si–B–C–N sample.

Table 3
Derived parameters from stress strain measurements (analysis with KWW equation, see text)

Material	Amorphous Si–B–C–N	Crystalline Si–B–C–N
ε_0	2.5×10^{-3}	2.6×10^{-3}
β	0.50	0.41
τ_{rel} (s)	2.8×10^{4}	3.6×10^{4}

ative of Eq. (5) yields the anelastic strain rate $\dot{\varepsilon}_{an}$, defined by the following equation:

$$\dot{\varepsilon}_{an}(T,t) = -\frac{\varepsilon_0\beta}{t}\cdot\left(\frac{t}{\tau_{rel}(T)}\right)^{\beta}\exp\left[-\left(\frac{t}{\tau_{rel}(T)}\right)^{\beta}\right]. \qquad (6)$$

For demonstration, this aforementioned procedure was used to fit the experimental anelastic strain data for the amorphous sample **V** and the nanocrystalline Si–B–C–N ceramics (sample **II**), as depicted in Fig. 9. The derived values of ε_0, β, and τ_{rel} for both samples are summarized in Table 3. It can be seen that the data for the amorphous and nanocrystalline Si–B–C–N ceramic are very similar. The relaxation times τ_{rel} in both systems are about 3×10^4 s, while the parameter β of the nanocrystalline Si–B–C–N ceramic implies a somewhat sharper relaxation time dispersion.

4. Discussion

4.1. Sample annealing, crystallization and structural characterization

Amorphous Si–B–C–N ceramics are metastable with respect to the crystalline phases of silicon nitride, silicon carbide, carbon and boron nitride [27]. However, the metastable state of these materials is characterized by a low atomic mobility, which prevents crystallization at lower temperatures. As a result, they only crystallize at temperatures above 1400 °C. If such amorphous materials are annealed at high temperatures, then various processes – comprising densification, crystallization and phase separation – might alter the sample structure. A similar phenomenon is observed in amorphous metallic glasses, if they are annealed at temperatures above the glass transition. Nevertheless, the structural stability of these ceramic materials and, consequently their respective mechanical properties, might be substantially improved by crystallization. It has been shown that after crystallization, β-SiC and eventually Si_3N_4 nanocrystallites are embedded in a turbostratic "B–C–N" matrix consisting of amorphous carbon and boron nitride domains [9]. Earlier studies on the crystallization of these materials have indicated that silicon carbide is the first phase to nucleate in the temperature range between 1400 and 1500 °C, whereas silicon nitride nucleates at and above 1700 °C [28]. Below 1350 °C the ceramic material was found to remain purely amorphous. The size of the SiC nanocrystallites was determined by high-resolution TEM studies, from which values between 2 and 5 nm were found [29].

It was observed that the crystallization kinetics directly depends on the actual annealing conditions. That is, the crystallization rate increases with increasing annealing temperature and time [28]. Likewise, the gas atmosphere plays an important role as well, which in particular holds for the impact of a nitrogen atmosphere [30]. For this reason the present amorphous Si–B–C–N ceramic was heat-treated at four different annealing conditions. The conditions (holding time, nitrogen pressure, temperature) were chosen in order to study the influence of these experimental parameters on the crystallization process.

It should be noted that so far no solid-state NMR studies exist for the structural evolution of Si–B–C–N ceramics after being subject to different annealing conditions at such high temperatures. At such high annealing temperatures of 1800 °C, in principle, two basic processes have to be distinguished: (i) sample decomposition via the reaction of Si_3N_4 with "free" (amorphous) carbon to form SiC and nitrogen [27], and (ii) crystallization of the amorphous ceramic material, i.e., demixing of the amorphous "Si–C–N"-matrix along with the formation of crystalline Si_3N_4 and SiC domains [27,31,32]. For the present discussion the demixing process is dominant, since sample decomposition is largely suppressed by the presence of a relatively high nitrogen pressure ($p_{N_2} \geqslant 10$ bar).

Thus, the experimental ^{13}C and ^{29}Si NMR spectra prove the presence of SiC (^{29}Si NMR signal at −18 ppm, ^{13}C NMR signal at 20 ppm), amorphous carbon (^{13}C NMR signal at 120 ppm), and Si_3N_4 (^{29}Si NMR signal at −48 ppm). For all samples the signal intensity of the SiC component is somewhat larger than that of the Si_3N_4 component, which qualitatively is in line with the X-ray observations. The NMR results for sample **II**, i.e., increase of the silicon carbide signal, loss of amorphous carbon signal, and reduction of silicon nitride signal intensity, suggest some decomposition during sample annealing. However, it should be noted that the relative ^{29}Si NMR signal intensities might not be completely correct. In highly crystalline Si_3N_4 very long spin-lattice relaxation times are expected, which for experimental reasons cannot always accounted for and which give rise to NMR signal saturation. Much more important, however, is the observed reduction of the ^{29}Si NMR line widths, which stems from an enhanced degree of crystallinity for sample **II**, i.e., the formation of larger nanocrystals.

The highest degree of crystallinity is thus registered for the sample exposed to a nitrogen pressure of 10 bar at 1800 °C for 3 h (sample **II**). At a higher nitrogen pressure of 100 bar silicon carbide and silicon

nitride domains are formed as well. However, relatively broad ^{29}S NMR line widths are registered, reflecting a lower degree of crystallinity for these samples, and the presence of the amorphous phase with mixed coordinated SiC_xN_{4-x} units ($x = 1$–4). In agreement with the corresponding X-ray diffraction and TEM studies, the present solid-state NMR data show that the highest degree of crystallinity is achieved by applying longer annealing times and lower nitrogen pressures.

On the basis of the derived ^{11}B NMR data it can be concluded that, during the silicon carbide formation and sample crystallization, distinct changes occur in the coordination sphere of the boron atoms. That is, a certain amount of the boron nuclei, that originally built up hexagonal BN domains, change their coordination from trigonal to tetragonal. Similar observations have been made during a previous NMR study on the same precursor system where the samples were annealed in an argon atmosphere [10]. However, so far no further detailed information about the constitution and structural changes within these BN domains is available.

In summary, the present annealed samples consist of hexagonal BN and graphite-like structures (''B–C–N'' matrix) with SiC and Si_3N_4 domains, from which, depending on the annealing conditions, SiC and Si_3N_4 nanocrystals emerge. We can further state that the degree of crystallinity increases in the following sequence sample **III** → sample **IV** → sample **I** → sample **II.** The present X-ray diffraction, TEM and solid-state NMR data independently demonstrate that a high nitrogen pressure of 100 MPa in general stabilizes the amorphous state, i.e., retards the crystallization of SiC and suppresses the formation of Si_3N_4 nanocrystals. Likewise, earlier extensive TEM studies have shown that holding times greater than 10 h at a given annealing temperature have only a marginal effect on the volume fraction of the produced nanocrystals [31]. In general, a nitrogen pressure of 10 bar was found to be completely sufficient to stabilize Si_3N_4 crystals. It was further concluded that an increasing nitrogen pressure provides no benefit, since it only retards the crystallization process. Thus, for the present Si–B–C–N ceramics, an annealing temperature of 1800 °C, a holding time of 3 h, and a nitrogen pressure of 10 bar provided a maximum amount of SiC and Si_3N_4 nanocrystals. These experimental results are qualitatively confirmed by thermodynamic calculations [33] which showed that the N_2 pressure is very crucial for the reaction of Si_3N_4 with carbon. A N_2 pressure of only 1 bar has thus practically no influence on the reactivity of Si_3N_4, whereas the transformation of Si_3N_4 is considerably retarded at higher nitrogen pressures.

4.2. Mechanical deformation at high temperatures

During the present work two types of high temperature compression tests were performed at a working temperature of 1400 °C, namely constant load experiments and load change experiments. Constant load experiments, with a load of 100 MPa, were performed on all annealed Si–B–C–N samples **I**–**IV**, and for comparison on an amorphous Si–B–C–N sample **V**. In general, an extraordinary high creep resistance could be detected for both types of materials. However, the deformation rates for the annealed Si–B–C–N ceramics (samples **I**–**IV**) were found to be an order of magnitude lower than those of the amorphous material throughout the whole testing period, implying a smaller total deformation of the former specimens (Fig. 5). It therefore can be concluded that a higher creep resistance emerges from the additional sample annealing at 1800 °C.

The time dependence of the deformation rate for the amorphous and nanocrystalline Si–B–C–N ceramics (Fig. 5) can be understood on the basis of a continuous structural evolution of the matrix phase during such experiments. Since the time dependence is rather similar, it is reasonable to assume that the matrix – consisting of well-defined but only partially crystalline SiC, Si_3N_4, BN domains and amorphous, graphite-like regions – plays the dominant role for the deformation behavior even of the crystalline Si–B–C–N ceramic rather than the dispersed nanocrystallites. In close analogy to the amorphous sample [8], it is the ongoing structural alteration in the amorphous matrix with testing time which is responsible for the continuous reduction of the deformation rate of the partially crystalline ceramics. The presence of isolated nanocrystallites obviously has a minor effect on the time dependence of the deformation or creep rate.

This is quite in contrast to the observations for partially crystalline metallic glasses where the effect of crystallization dominates the creep behavior [18]. The creep rates were found to decrease by several orders of magnitude in annealed metallic glasses, where continuous crystallization was observed in prolonged creep experiments at high temperatures. The strong reduction of the creep rate from its initial value was mainly attributed to the in situ formation of crystallites in such metallic glasses. It was further observed that the creep rates of completely crystalline specimens do not drop down any further, and reach a constant limiting value [18]. In the case of the present annealed Si–B–C–N ceramics, the structural evolution of the amorphous phase is not yet completed, not even after a very long time. Thus, structural changes in the amorphous B–C–N matrix still go on along with sample crystallization during the entire time of the creep experiments. This is also consistent with the absence of any asymptotic behavior even after 300 h of testing time. The fact that the crystallization rate in Si–B–C–N ceramics is much smaller than in metallic glasses also supports the hypothesis of a minor influence of nanocrystallites on the enhanced creep resistance of the annealed Si–B–C–N ceramics. A finite contribution

from the nanocrystallites, nevertheless, cannot be completely ruled out.

The viscosities of amorphous and nanocrystalline Si–B–C–N ceramics derived from load change experiments were found to be very similar with values between 10^{15} and 10^{16} Pa s. These values are about six orders of magnitude higher than those discussed for fused silica in the temperature range from 1400 to 1500 °C [34], reflecting in general a high mechanical stability of the more covalent Si–B–C–N materials. Moreover, the four annealed samples **I**–**IV** exhibit somewhat higher viscosities (about one order of magnitude) than the amorphous sample **V**, which can be traced back to the structural differences between the amorphous and annealed samples (i.e., "BCN"-matrix, Si_3N_4 and SiC domains), as already outlined above.

Earlier studies showed that the fitting parameters β and τ_{rel} (Eq. (6)) are practically independent of the applied stress. At the same time the pre-exponential constant ε_0 exhibited a pronounced stress dependence, which is reflected by a linear variation with stress change [35]. In the present study, no further attempts were made to relate these fitting parameters to the applied stress. The stretching exponent β is known to be directly connected with the structural relaxation of these materials, and will be discussed next.

Stretching exponents β of 0.6 for amorphous $Ni_{0.5}Zr_{0.5}$ [21], 0.43 for C_{60} [22], 0.42 for amorphous silicon [23], 0.4–0.6 for various polymers [24], and 0.47 for amorphous Si–C–N ceramics [35] have been reported in the literature. It is found that practically all published values for the stretching exponent β lie between 0.4 and 0.6. Phillips et al. [36,37] explained these stretching exponents by a trap model, which is based on the idea that in glasses a static distribution of traps or sinks exists towards which excitations diffuse and disappear [38]. The value of the stretching exponent is then given by

$$\beta = \frac{d}{(d+2)}, \tag{7}$$

where d is the dimensionality of the configuration space in which the relaxation takes place. For a three-dimensional distribution, Eq. (7) yields a value of $\beta = 0.6$ which reproduces the stretching exponents observed for some of the glasses, but not for all materials. By comprising long range forces, namely the Coulomb forces, a new dimensionality was formulated with $d = 3/2$. From this, a stretching exponent of $\beta = 3/7 = 0.43$ was derived which is much closer to the value found experimentally for the annealed, nanocrystalline Si–B–C–N ceramics of the present study (Table 3). According to this model, Coulomb forces would govern the observed relaxation processes in addition to density fluctuations. The experimental stretching exponent $\beta = 0.5$ derived for the amorphous Si–B–C–N sample **V** is neither close to 0.43 nor to 0.6. In this context, it is interesting to note that the published stretching exponents for stress relaxation in oxide glasses are also about 0.5 for a wide range of compositions [26], which therefore also cannot be completely reproduced on the basis of the existing theoretical models.

5. Conclusions

A detailed investigation has been carried out on the crystallization behavior of amorphous Si–B–C–N ceramics. Part of the present work focused on the effects of temperature, holding time and nitrogen pressure on the structural changes during crystallization. The analysis of the solid-state NMR, X-ray diffraction and TEM experiments clearly demonstrated that at the chosen annealing temperature of 1800 °C both the nitrogen gas pressure and the exposure time have a strong impact on the actual molecular constitution. It was found that a maximum of sample crystallinity is achieved by annealing for 3 h at a nitrogen pressure of 10 bar.

During constant load and load change deformation experiments at 1400 °C, the nanocrystalline, annealed Si–B–C–N ceramic samples were found to exhibit a higher creep resistance than the corresponding amorphous sample, while the actual time dependence of the creep rates – including the absence of any asymptotic behavior – was practically identical for both materials. It is thus anticipated that it is the viscous flow of the B–C–N matrix and its change with time at the testing temperature which governs the creep behavior in nanocrystalline Si–B–C–N ceramics. The role of the nanocrystallites is obviously of minor importance for the mechanical properties examined here.

Acknowledgment

Financial support for this project by the Deutsche Forschungsgemeinschaft is gratefully acknowledged.

References

[1] Bill J, Aldinger F. Precursor-derived covalent ceramics. In: Bill J, Wakai F, Aldinger F, editors. Precursor-derived ceramics. Weinheim: Wiley-VCH; 1999. p. 33.
[2] Bill J, Aldinger F. Adv Mater 1995;7:775.
[3] Riedel R, Kienzle A, Dreßler W, Ruswisch LM, Bill J, Aldinger F. Nature (London) 1996;382:796.
[4] Weinmann M, Schuhmacher J, Kummer H, Prinz S, Peng J, Seifert HJ, et al. Chem Mater 2000;12(3):623.
[5] Wang ZC, Aldinger F, Riedel R. J Am Ceram Soc 2001;84(10):2179.
[6] Müller A, Gerstel P, Weinmann M, Bill J, Aldinger F. J Eur Ceram Soc 2001;21:2171.
[7] Thurn G, Aldinger F. Compression creep behaviour of precursor-derived ceramics. In: Bill J, Wakai F, Aldinger F, editors. Precursor-derived ceramics. Weinheim: Wiley-VCH; 1999. p. 237.

[8] Christ M, Thurn G, Weinmann M, Bill J, Aldinger F. J Am Ceram Soc 2000;83(12):3025.
[9] Christ M, Zimmermann A, Zern A, Weinmann M, Aldinger F. J Mater Sci 2001;36:5767.
[10] Schuhmacher J, Berger F, Weinmann M, Bill J, Aldinger F, Müller K. Appl Organomet Chem 2001;15(10):809.
[11] Schuhmacher J, Weinmann M, Bill J, Aldinger F, Müller K. Chem Mater 1998;10:3913.
[12] Hartman JS, Richardson MF, Sheriff BL, Winsborrow BG. J Am Chem Soc 1987;109:6059.
[13] Carduner KR, Carter III RO, Milberg ME, Crosbie GM. Anal Chem 1987;59:2794.
[14] Marchetti PS, Kwon D, Schmidt WR, Interrenate LV, Maciel GE. Chem Mater 1991;3:482.
[15] Christ M, Thurn G, Bill J, Aldinger F. High temperature mechanical properties of Si–B–C–N precursor-derived amorphous ceramics. In: Müller G, editor. Ceramics-processing, reliability, tribology and wear, Euromat. Weinheim: Wiley-VCH; 2000. p. 359.
[16] Wainuk TA, Busch R, Masuhr A, Johnson WL. Acta Mater 1998;46(15):5229.
[17] Anderson PM, Lord AE. Mater Sci Eng 1980;44:279.
[18] Patterson JP, Jones DRH. Acta Metall 1980;28:675.
[19] Christ M, Zimmermann A, Aldinger F. J Mater Res 2001;16(7):1994.
[20] Kohlrausch R. Ann Phys (Leipzig) 1847;12:393.
[21] Teichler H. Phys Stat Sol (b) 1992;172:325.
[22] Cheville RA, Halas NJ. Phys Rev B 1992;45(8):4548.
[23] Kakailios J, Street RA, Jackson WB. Phys Rev Lett 1987;59:1037.
[24] Böhmer R, Ngai KL, Angell CA, Plazek DJ. J Chem Phys 1993;99:4201.
[25] Williams G, Watts DC. Trans Faraday Soc 1970;66:80.
[26] Scherrer GW. Relaxation in glass and composites. New York (NY): Wiley; 1986.
[27] Peng J, Seifert HJ, Aldinger F. Ceram Trans 2000;115:251.
[28] Janakiraman N, Weinmann M, Schuhmacher J, Müller K, Bill J, Aldinger F, et al. J Am Ceram Soc 2002;85(7):1807.
[29] Cai Y, Zimmermann A, Prinz S, Zern A, Phillip F, Aldinger F. Scr Mater 2001;45(11):1301.
[30] Cai Y, Zimmermann A, Prinz S, Aldinger F. J Mater Res 2002;17(11):2765.
[31] Aldinger F, Prinz S, Janakiraman N, Kumar R, Christ M, Weinmann M, et al. Int J Self-Prop High-Temp Syn 2001;10(3):249.
[32] Bill J, Kamphowe TW, Müller A, Wichmann T, Zern A, Jalowieki A, et al. Appl Organomet Chem 2001;15:777.
[33] Peng J. Thermochemistry and constitution of precursor-derived Si–(B–)C–N ceramics. PhD Thesis, University of Stuttgart; 2002.
[34] Kingery WD, Bowen HK, Uhlmann DR. Introduction to ceramics. 2nd ed. New York (NY): Wiley; 1976.
[35] Bauer A, Christ M, Cai Y, Zimmermann A, Aldinger F. J Am Ceram Soc [accepted]
[36] Phillips JC. J Non-Cryst Solids 1994;172–174:98.
[37] Phillips JC. J Non-Cryst Solids 1995;182:155.
[38] Grassberger P, Procaccia I. J Chem Phys 1982;77:6281.